View metadata, citation and similar papers at core.ac.uk
brought to you by CORE
provided by CiteSeerX

Molecular Simulation
Vol. 37, No. 10, September 2011, 855–864

Taylor & Francis
Taylor & Francis Group

A molecular dynamics boundary condition for heat exchange between walls and a fluid

E.A.T. van den Akker[a]*, A.J.H. Frijns[a], P.A.J. Hilbers[b] and A.A. van Steenhoven[a]

[a]*Department of Mechanical Engineering, Eindhoven University of Technology, Eindhoven, The Netherlands;* [b]*Department of Biomedical Engineering, Eindhoven University of Technology, Eindhoven, The Netherlands*

(*Received 21 July 2010; final version received 23 February 2011*)

In molecular dynamics simulations of heat transfer in micro channels, a lot of computation time is used when the wall molecules are explicitly simulated. To save computation time, implicit boundary conditions, such as the Maxwell conditions, can be used. With these boundary conditions, heat transfer is still a problem. In this work, we derive a new boundary condition based on a vibrating potential wall. The heat-transfer properties of the new boundary condition are shown to be comparable with those of the explicit wall. The computation time needed for the implicit boundary condition is very small compared with that needed for the explicit simulation.

Keywords: micro/nano channel; thermal boundary condition; molecular dynamics

Downloaded by [Eindhoven Technical University] at 00:39 07 October 2011

1. Introduction

Computer chips of last decades have become more powerful and smaller in size [1]. As a consequence of this technological improvement, the heat produced per area by a computer chip has increased, and is expected to increase further [2]. A conventional way to remove this heat is by air cooling, but the limits of air cooling are being reached.

Micro-channel cooling is a promising way to solve the cooling problem for computer chips. In micro-channel cooling, a fluid flows through a micro channel in close contact with the computer chip. Owing to the large area to volume ratio of the micro channel, the amount of heat removed is larger than by conventional air cooling. Heat transfer by forced convection for gases is in the range of $25-250\,\mathrm{kW\,m^{-2}}$ [3], whereas experimental micro channels with water have shown a heat flux of $500\,\mathrm{kW\,m^{-2}}$ [4]. The heat removal is optimal when evaporation takes place in the micro channel [5]. To optimise micro-channel configurations, the heat and flow problems in the micro channel need to be understood, including the heat transfer between the channel wall and the fluid.

Because of the small size of the micro channel, the continuum approximation is not valid in the gas phase [6]. This means that evaporation, an important contributor to heat removal, cannot be analysed with continuum techniques. Other techniques, which include the particle nature of the fluids, should be used to study evaporation and condensation in the micro channel. One of these methods is molecular dynamics (MD) [7,8]. In MD, the trajectories of the particles are calculated by analysing the interactions between all particles. It is possible to explicitly include wall particles in the MD simulation. Explicit walls are expected to give the best results, but at the price of high computational costs. Because several layers in the wall need to be calculated, the number of particles in the wall may be larger than the number of particles in the fluid, so the majority of the computation time is needed for the simulation of the wall particles.

A solution to the computation-time problem in the simulation of explicit walls is to fix the position of the wall particles and to only simulate their influence on fluid particles. Although this is time saving, there is no energy exchange from the fluid particles to the wall particles, so the heat transfer between the fluid and the wall is impossible.

To replace the explicit wall with a computationally less expensive method that is capable of handling heat transfer, an implicit boundary condition originating from vibrating walls is derived. This boundary condition is shown to work for walls with a continuous potential energy function, for example the Lennard-Jones potential, as well as for walls with a discontinuous potential, for example the hard-sphere potential. The resulting power input by the vibrating wall corresponds to granular theory.

2. Theory

2.1 *Vibrating wall*

In MD, the motion of particles is simulated, dealing with the interactions by means of a force between the particles that are derived from their potential energy *V*. MD simulations work for gases, liquids and solids. MD can be used to simulate micro channels, in which heat is transferred from the solid wall to the fluid inside the micro channel.

*Corresponding author. Email: e.a.t.v.d.akker@alumnus.tue.nl

ISSN 0892-7022 print/ISSN 1029-0435 online
© 2011 Taylor & Francis
DOI: 10.1080/08927022.2011.566694
http://www.informaworld.com

Downloaded by [Eindhoven Technical University] at 00:39 07 October 2011

The wall particles, positioned in an *fcc*-lattice, are vibrating due to their thermal motion, as shown in Figure 1(a). Because of the computational effort needed to simulate this thermal motion, methods have been developed to replace the explicit wall by a computationally cheaper solution. The Maxwell model [9] is a commonly used model, but the accommodation coefficient in that model is not a priori known [10]. We follow a different approach here, in which a particle moving towards a wall interacts with a small part of the wall, as if the wall particles are one rigid vibrating body, as shown in Figure 1(b). The interacting part of the wall is vibrating as if it is connected with a spring with spring constant k_w. If a (section of the) wall is vibrating with total energy E_w, mass M_w and wall spring constant k_w, and interaction with fluid particles can be neglected, the position y of the wall is given as

$$y(\varphi) = \sqrt{\frac{2E_w}{k_w}}\cos(\varphi), \quad \varphi = \sqrt{\frac{k_w}{M_w}}t, \tag{1}$$

where φ is the phase.

The spring constant k_w is estimated by looking at an explicit wall. For example, in the case of a wall made of calcium atoms in an *fcc*-lattice, all neighbouring particles vibrate around the equilibrium distance of $2^{1/6}\ \sigma_{\mathrm{Ca}}$ (with σ_{Ca} being the atomic diameter of calcium). A Taylor expansion shows that the interaction is approximated as a spring with spring constant $k_w = 2^{2/3}\varepsilon_{\mathrm{Ca}}/\sigma_{\mathrm{Ca}}^2 \approx 300\varepsilon_{\mathrm{Ar}}/\sigma_{\mathrm{Ar}}^2$; the total spring constant is of the same order [11]. The wall energy E_w (the potential and kinetic energy of the interacting part of the wall) is of the order of $\varepsilon_{\mathrm{Ar}}$. This means that the amplitude of the vibration, calculated from (1), is $\sqrt{2E_w/k_w} \approx 0.1\ \sigma_{\mathrm{Ca}}$, so the wall vibrations are relatively small. The velocity of the wall v_w is

$$v_w(\varphi) = -\sqrt{\frac{2E_w}{M_w}}\sin(\varphi), \tag{2}$$

which shows that the magnitude of the velocity is independent of the spring constant k_w.

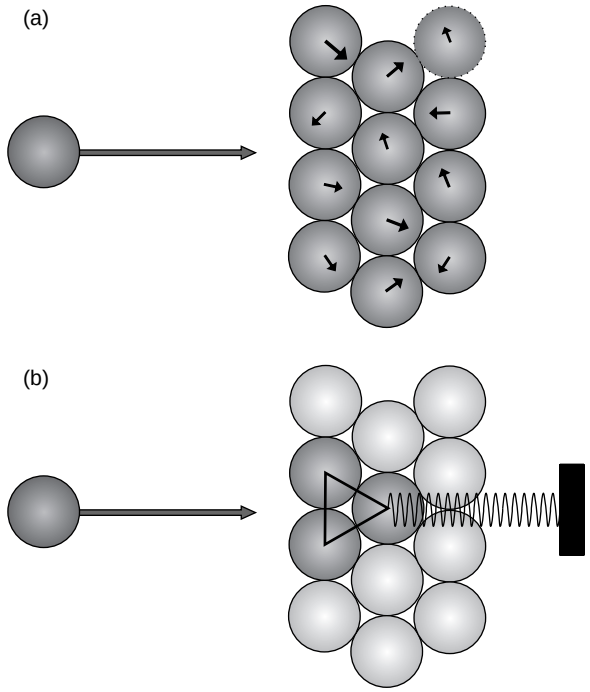

Figure 1. Interaction between a particle and a wall. In panel (a), the explicit wall interaction is shown, in which inside the wall, all interactions are calculated, and all particles can have different velocities. The interaction between a particle and part of a wall seen as a rigid vibrating body is shown in panel (b). There, during the collision, the other particles (here in lighter colour) are ignored.

2.2 Collision model

In MD, the interaction between particles is specified by a potential energy function, giving the potential energy V due to the interaction of two particles at distance r. The commonly used potential energy function is the Lennard-Jones potential [7,8,12]. Other potentials can also be used for the interaction between a fluid particle and a solid wall, for example the Stillinger–Weber potential [13]. Further on, the Lennard-Jones potential is used as an example; the calculations for other continuous potentials are similar. As an example for a non-continuous potential, the hard-sphere potential is used. For both types of potentials, the collision between a fluid particle and the wall is analysed.

2.2.1 Collision with a potential wall

If the interaction between a fluid particle and the wall is modelled with a potential energy function V, the force between the two particles F is given as $F = -V'(x) = \partial V/\partial\vec{x}$. According to Newton's second law, the differential equation for the position of the particle x is given by

$$\frac{\mathrm{d}^2x}{\mathrm{d}t^2} = -\frac{V'(x-y)}{m}, \tag{3}$$

where m is the mass of the particle and y is the position of the wall. The motion of the wall is determined by the force between the wall and the particle, and the force of the spring. If the spring has spring constant k_w, then the differential equation for the position y of the wall is given by

$$\frac{\mathrm{d}^2y}{\mathrm{d}t^2} = \frac{V'(x-y) - k_w y}{M_w}, \tag{4}$$

where M_w is the mass of the part of the wall involved in the interaction. Here, the part of the wall involved in the

Downloaded by [Eindhoven Technical University] at 00:39 07 October 2011

interaction is seen as one bigger and heavier wall particle. The first right-hand term corresponds to the fluid–wall interaction and the second to the spring–wall interaction.

2.2.2 *Collision with a reflective wall*

In the case of a non-continuous potential such as the hard sphere, the velocities of the particle and wall change instantly. If a particle with mass m and velocity perpendicular to the wall v_x hits the wall when the wall has a velocity v_w, conservation of momentum and kinetic energy determines that the velocities v_w^* and v_x^* directly after the collision, are

$$\begin{aligned} v_w^* &= \frac{2}{1+\mu} v_x - \frac{1-\mu}{1+\mu} v_w, \\ v_x^* &= \frac{1-\mu}{1+\mu} v_x + \frac{2\mu}{1+\mu} v_w, \end{aligned} \tag{5}$$

where $\mu = M_w/m$. The wall speed before the collision v_w depends, according to Equation (2), on the phase φ of the wall at the moment of collision. Not every phase has the same probability; the particle is less likely to interact with the wall if the wall is moving away from an impending particle, and is more likely to interact with the wall if the wall is moving towards the particle. Two situations can be distinguished by the relative velocity v_r, given by

$$v_r = -\frac{v_x}{v_w^{\mathrm{MAX}}} = -v_x \sqrt{\frac{M_w}{2E_w}}, \tag{6}$$

with v_w^{MAX} being the maximal velocity of the wall as seen from (2). If v_r is larger than 1, the situation is as shown in Figure 2(a): the particle is always moving faster than the wall, and the wall can be hit in every phase, although not all phases have the same probability.

The probability that the first impact happens before phase φ^* is equal to the probability that at time zero, when the wall position is maximal, the particle is closer to the wall than the position that would result in an impact at phase φ^*. At the last instant when the wall position is maximal before the collision, the particle is between dimensionless positions 1 and $1 + 2\pi v_r$. Because it is before the collision, every position is equally probable, so uniformly distributed, so the probability that the impact happens before phase φ^* has the cumulative distribution function given by

$$\begin{aligned} P(\varphi < \varphi^*) &= P\big(\cos(\varphi) + \varphi \ v_r < \cos(\varphi^*) + \varphi^* v_r\big) \\ &= \frac{\cos(\varphi^*) + \varphi^* v_r}{2\pi v_r}. \end{aligned} \tag{7}$$

Therefore, the probability density function p of impact at phase φ is given by

$$p(\varphi) = \frac{1}{2\pi} - \frac{\sin(\varphi)}{2\pi v_r}. \tag{8}$$

This is only the probability for the first collision; it can happen that when a particle approaches the wall, there are multiple collisions, as depicted in Figure 3. This will be dealt with later.

If v_r is smaller than 1, the situation is as depicted in Figure 2(b): the particle is sometimes moving slower than the wall, and when the wall is moving backwards faster than the particle is moving forwards, the wall cannot be hit in that phase. The 'critical path' that separates the accessible from the inaccessible phases is given by

$$x(\varphi) = \cos(\arcsin(v_r)) + v_r\big(\arcsin(v_r) - \varphi\big), \tag{9}$$

so phase φ is accessible if

$$\cos(\varphi) + v_r\varphi > \cos(\arcsin(v_r)) + v_r \arcsin(v_r). \tag{10}$$

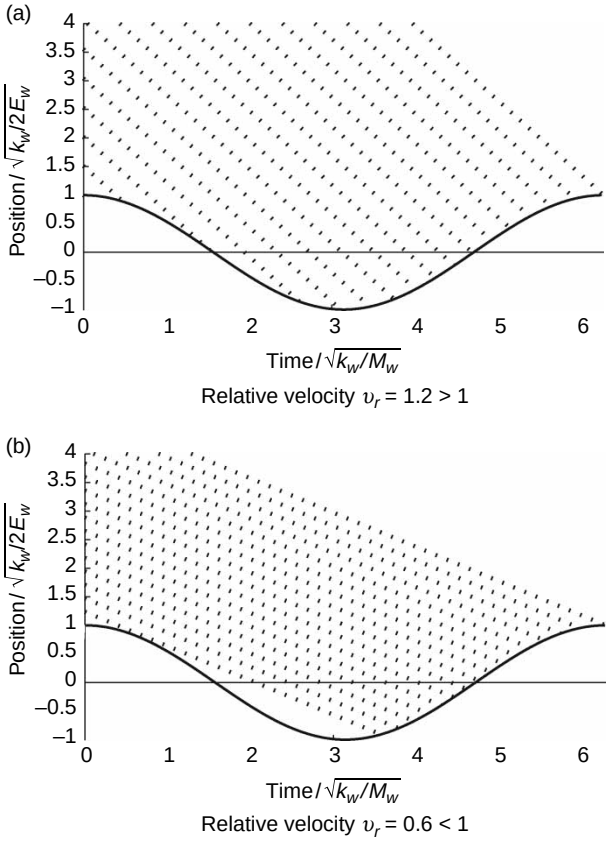

Figure 2. Possible paths for a particle (dotted lines) with a relative velocity larger than 1 (panel a) and smaller than 1 (panel b), colliding with a vibrating wall (solid line). If the relative velocity is larger than 1, the wall can always be hit by a particle, which means that every phase is accessible. The collision is more probable when the wall is moving towards the particle. If the relative velocity is smaller than 1, not every phase is accessible.

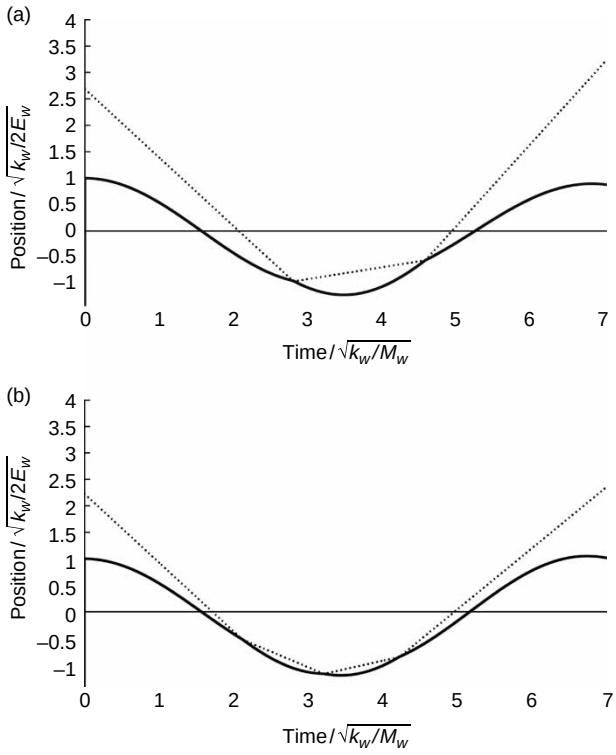

Figure 3. The trajectories of the vibrating wall (solid line) and an incoming particle (dashed line), colliding two times (left image) and three times (right image). In both pictures, the mass ratio $\mu = 3.6$ and the relative velocity before the collision $v_r = 1.3$.

The probability of collision at phase φ when $v_r < 1$ is analysed in the same way as when $v_r > 1$, with the same result: if phase φ is accessible, the probability $p(\varphi)$ of a collision at phase φ is also given by (8). This is also only valid for the first collision; if a particle collides multiple times with the wall (similar to Figure 3), the total energy exchange between wall and particle increases, and phase probabilities become more complicated.

From (2) and (5) it is seen that the minimum velocity of a particle after a single collision is

$$\min(v_x^*) = \frac{1-\mu}{1+\mu} v_x - \frac{2\mu}{1+\mu}\sqrt{2\frac{E_w}{M_w}}, \tag{11}$$

and the maximum velocity of the wall after the collision is

$$\max(v_w^*) = \sqrt{2\frac{E_w + \Delta E}{M_w}} \approx \sqrt{2\frac{E_w}{M_w}}, \tag{12}$$

where ΔE is the exchanged energy during the collision, typically small compared with E_w. If the minimal velocity of the particle after the collision is larger than the maximal velocity of the wall after the collision, they will never collide for a second time:

$$v_r = -v_x\sqrt{\frac{M_w}{2E_w}} > \frac{1+3\mu}{1-\mu}. \tag{13}$$

If the relative velocity is smaller than this, multiple collisions may occur.

2.3 Energy exchange

During the interaction between a fluid particle and the wall, energy is exchanged. When the wall potential is discontinuous, as the hard-sphere potential, this energy is exchanged instantaneously, but if the potential is continuous, the energy exchange takes some time and is more complicated to be determined.

2.3.1 Energy exchange with potential wall

From a dimensional analysis of the problem, three dimensionless parameters are extracted:

$$\delta = \sqrt{\frac{2E_w}{k_w\sigma^2}}, \quad \lambda = \frac{1/2mv_0^2 + V(x_0)}{k_B T_w}, \quad \text{and} \quad \mu = \frac{M_w}{m}, \tag{14}$$

where k_B is Boltzmann's constant for the interaction between a wall and a particle at position x_0 with velocity v_0. Here, δ can be interpreted as the dimensionless wall amplitude directly related to the temperature, λ is the ratio of energies of the particle and the wall, and μ is the mass ratio between the particle and the part of the wall that is involved in the interaction. From the literature [14], a value of $\mu = 3.6$ is shown to be reasonable in similar problems, and is assumed here. The total energy of the particle E_p (kinetic and potential) is a function of these three dimensionless parameters δ, λ and μ, the initial phase of the wall φ_0 and the time t, so

$$E_p = E_p(t; \delta, \lambda, \mu, \varphi_0). \tag{15}$$

The mean exchanged energy during a collision is defined as the difference between the total energy of the particle before and after the collision, averaged over the initial wall phases φ_0, so

$$\Delta E(\delta, \lambda, \mu) = \frac{1}{2\pi}\int_0^{2\pi} \big(E_p(t_0; \delta, \lambda, \mu, \varphi_0) - E_p(t_1; \delta, \lambda, \mu, \varphi_0)\big)\mathrm{d}\varphi_0, \tag{16}$$

where t_0 is the time before the collision and t_1 is the time directly after the first collision. After the first collision between a fluid particle and an explicit wall, internal wall vibrations will influence the outer wall behaviour and the

Downloaded by [Eindhoven Technical University] at 00:39 07 October 2011

model in Section 2.2 will not be accurate anymore, so the collisions after the first collision are ignored. Here, a linear approximation of the exchanged energy in δ and λ is used,

$$\Delta E(\delta, \lambda, \mu) \approx \Delta E(\delta_0, 0, \mu) + \left[\frac{\partial \Delta E}{\partial \delta}\right]_\lambda (\delta - \delta_0) + \left[\frac{\partial \Delta E}{\partial \lambda}\right]_\delta \lambda, \tag{17}$$

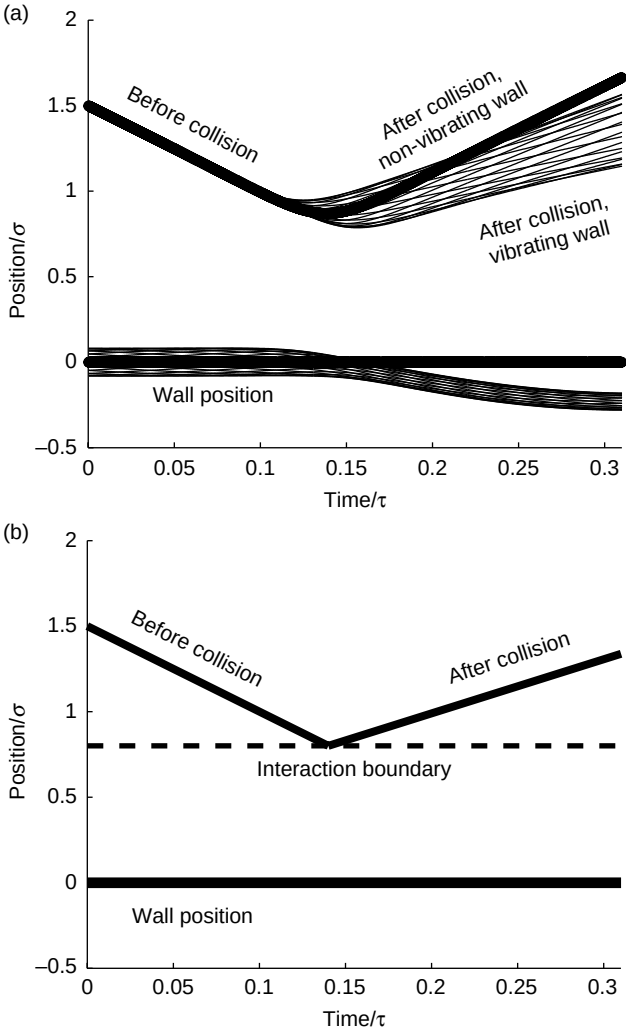

Figure 4. Left panel: The motion of a particle (upper lines) hitting a vibrating wall (lower lines), as the numerical solution of (3) and (4), with initial conditions (22), where $x_0 = 1.5\,\sigma$, $v = 5\,\sigma/\tau$ and $E_w = \varepsilon$. The different small lines are the results for different initial phases of the wall φ_0. Also shown as the thick line is the solution for a non-vibrating wall. Right panel: The new model, based on Figure 4(a). A particle moving towards the wall is not influenced by the wall until it crosses the interaction boundary, at a distance $0.8\,\sigma$ of the wall. At that moment energy is exchanged according to (24), and the particle is reflected with the velocity according to the new energy.

with $[\partial \Delta E/\partial \delta]_\lambda$ and $[\partial \Delta E/\partial \lambda]_\delta$ are constants. Furthermore, δ_0 corresponds to the dimensionless wall amplitude corresponding to a typical temperature of the problem, and $\lambda = 0$ corresponds to a particle that almost escapes from the wall.

In our approach, Equation (17) is taken as a starting point. In the exact situation, as shown in Figure 4(a), a particle close to the wall interacts with the wall over a short period of time, with an energy change that depends on the initial phase of the wall φ_0. In the new model, as shown in Figure 4(b), the particle is not influenced by the presence of the wall until it crosses the 'interaction boundary' of the wall. At that moment, the energy exchange according to (17) takes place, and the particle reverses its direction. The 'interaction boundary', found from examining situations as shown in Figure 4(a), is put at 0.8σ from the wall. This is approximately the distance at which the kinetic energy from the particle is completely changed into potential energy, adjusted for the small distance that the wall moves. This distance is slightly dependent on the energy of the particle, but this small influence is ignored in the analysis, as it will not influence the results much. Hence, the distance of 0.8σ is used for all interactions.

In this boundary condition, three parameters have to be specified: $\Delta E(\delta_0, 0, \mu)$, $[\partial \Delta E/\partial \delta]_\lambda$ and $[\partial \Delta E/\partial \lambda]_\delta$. Two of them are found by analysing the situation of an ideal gas in contact with the boundary condition. In the model as shown in Figure 4(b), the potential energy contribution from the wall is neglected, so the dimensionless parameter $\lambda = E_{\text{kin}}/k_{\text{B}}T_w$, where E_{kin} is the kinetic energy of the particle. The kinetic energy $E_{\text{kin}} = 1/2\, mv^2$ of an ideal gas particle with temperature T_g passing through a plane, normal to that plane, is distributed according to Ref. [15]

$$p(E_{\text{kin}}) = \frac{1}{k_{\text{B}}T_g}\exp\left(-\frac{E_{\text{kin}}}{k_{\text{B}}T_g}\right), \quad \text{so}$$
$$p(\lambda) = \frac{T_w}{T_g}\exp\left(-\lambda\frac{T_w}{T_g}\right). \tag{18}$$

With this distribution, the expected energy exchange $\mathcal{E}[\Delta E]$ between a wall with temperature T and an ideal gas with temperature T is

$$\mathcal{E}[\Delta E] = \int_0^\infty \Delta E(\lambda) p(\lambda) \mathrm{d}\lambda = \Delta E(\delta_0, 0, \mu) + \left[\frac{\partial \Delta E}{\partial \delta}\right]_\lambda (\delta - \delta_0) + \left[\frac{\partial \Delta E}{\partial \lambda}\right]_\delta. \tag{19}$$

If the wall and the gas have the same temperature T, on average no heat is exchanged [16], so $\mathcal{E}[\Delta E] = 0$. This

Downloaded by [Eindhoven Technical University] at 00:39 07 October 2011

Downloaded by [Eindhoven Technical University] at 00:39 07 October 2011

holds for every value of δ, so

$$\left[\frac{\partial \Delta E}{\partial \delta}\right]_{\lambda} = 0 \quad \text{and} \quad \Delta E(\delta_0, 0, \mu) = -\left[\frac{\partial \Delta E}{\partial \lambda}\right]_{\delta}. \tag{20}$$

This shows that ΔE is independent of δ, and the problem is reduced to finding the coefficient $[\partial \Delta E/\partial \lambda]_{\delta}$. This is estimated first by treating the energy transfer as instantaneous. In that case, the transferred energy found from the conservation of energy and momentum is (see also (25)) given by

$$\begin{aligned} \Delta E_{\text{inst}} &= -2E_w \frac{1 - 2\mu + 2\lambda\mu}{(1+\mu)^2}, \quad \text{so} \\ \left[\frac{\partial(\Delta E_{\text{inst}})}{\partial \lambda}\right]_{\delta} &= -\frac{4\mu}{(1+\mu)^2} E_w. \end{aligned} \tag{21}$$

Because the energy transfer is not instantaneous, (21) is not exact for the potential wall, but the coefficient is still expected to be proportional to the wall energy E_w, and for the rest dependent on the mass ratio μ only. The coefficient $[\partial \Delta E/\partial \lambda]_{\delta}$ was found from MD simulations. The temperature in problems of interest typically varies from 0.5 to 2.0 ε/k_{B} (corresponding to temperatures between 60 and 240 K for Argon), so $0.1 < \delta < 0.2$. Because in practical situations the temperature of the wall and the fluid in contact with the wall will be similar, λ will be around 1 according to (14); here, λ is sampled from random distribution (18). In this parameter region, one-dimensional (1D) MD simulations were performed, solving the equations of motion from Section 2.2. The initial conditions are given as

$$\begin{aligned} &x[0] = x_0, \quad x'[0] = v, \\ &\frac{k_w}{2} y[0]^2 + \frac{M}{2} y'[0]^2 = E_w, \\ &y[0] = \sqrt{\frac{2E_w}{k_w}} \cos(\varphi_0), \end{aligned} \tag{22}$$

where φ_0 is the initial phase of the wall, $0 \le \varphi_0 < 2\pi$. These equations were solved numerically in a 1D MD simulation using the leap-frog algorithm [8]. The result for initial conditions, $x_0 = 1.5\,\sigma$, $v = 5\,\sigma/\tau$ and $E_w = \varepsilon$ (where σ, τ and ε are the length scale, time scale and energy scale of the Lennard-Jones potential, respectively) and various initial phases of the wall φ_0 is shown in Figure 4(a), together with the solution for a non-vibrating wall. If a particle hits a non-vibrating wall, no energy is exchanged: the outgoing velocity is equal to the incoming velocity. The solution in which the particle hits a vibrating wall clearly shows lower outgoing velocities; this shows that during the interaction, energy was transferred from the particle to the wall.

The remaining coefficient in (20) was fitted as

$$\left[\frac{\partial \Delta E}{\partial \lambda}\right]_{\delta} = (-0.531 \pm 0.01) E_w. \tag{23}$$

In comparison, the estimated coefficient from (21) with $\mu = 3.6$ is $\left[\partial \Delta E/\partial \lambda\right]_{\delta} = -0.68\,E_w$. The result of the fit is shown in Figure 5.

There is a small probability that a particle with high energy ($\lambda > 5$) interacts with the wall. According to (13), this particle interacts in a single collision, and approximation (21) still holds, so no deviation from the fit in Figure 5 is expected. Combining the above results, the relation for the exchanged energy during a collision, used in the model, is

$$\Delta E(\delta, \lambda, \mu) = 0.531(1 - \lambda) E_w. \tag{24}$$

Directly after the collision of a particle with the wall, the part of the wall involved in the collision has a different energy level than the rest of the wall; because the time scale for heat conduction in a solid is much smaller than between a solid and a gas [17], in the model the energy is immediately redistributed over the wall.

2.3.2 *Exchanged energy with reflective wall*

The dimensionless parameters δ, λ and μ from (14) are used here too. The energy transferred from the wall to the particle in this single collision ΔE is directly found from (5) as

$$\begin{aligned} \Delta E &= \frac{m}{2}\left(v_x^{*2} - v_x^2\right) \\ &= -\frac{2m\mu(v_x - v_w)(v_x + \mu v_w)}{(1+\mu)^2}. \end{aligned} \tag{25}$$

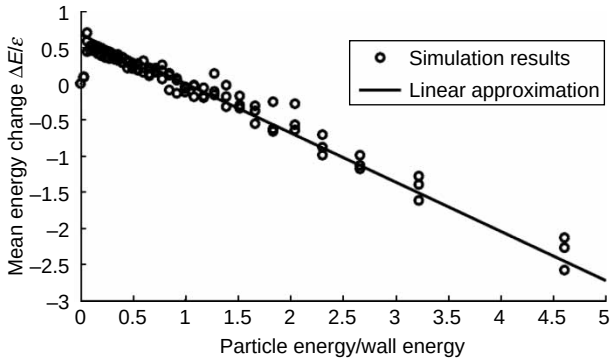

Figure 5. Shown in dots is the exchanged energy during the first collision, for several values of $\delta (0.1 < \delta < 0.2)$, between a particle and a vibrating wall for varying λ, and $\mu = 3.6$ fixed, found from MD simulations. The linear approximation with $[\partial \Delta E/\partial \lambda]_{\delta} = -0.531\,E_w$ is shown with a line.

Downloaded by [Eindhoven Technical University] at 00:39 07 October 2011

In this case, when only simple collisions can occur, the probability of the impact phase is as given in (8). The expected value of the exchanged energy $\mathcal{E}[\Delta E]$ can, therefore, be calculated as

$$\mathcal{E}[\Delta E] = \int_0^{2\pi} \Delta E(\varphi) p(\varphi) \mathrm{d}\varphi = -2E_w \frac{1 + 2v_r^2 - 2\mu}{(1+\mu)^2}$$
$$= -2E_w \frac{1 - 2\mu + 2\lambda\mu}{(1+\mu)^2}, \qquad (26)$$

where λ is the same as in (14). This expected value is not only exact for single collisions but also a good approximation for multiple collisions, as shown in Figure 6. There, the exchanged energy $\mathcal{E}[\Delta E]$ predicted by (26) is compared with simulation results. In these simulations, for different relative velocities v_r, many particles were simulated which collide with a reflective vibrating wall.

For relative velocities $0.5 < v_r < 3.5$, the number of collisions per interaction can be more than 1, so the mean exchanged energy is higher than the energy given by (26), but from the figure it is seen that the difference is never large. If the relative velocity v_r is close to 0 ($0 < v_r < 0.5$), not all phases are accessible although the calculation still assumes it, and the energy exchange is overestimated.

Although the prediction for the mean exchanged energy $\mathcal{E}[\Delta E]$ is not exact, it is accurate enough to be used for the new wall model that uses this mean exchanged energy for every interaction, such that the phase φ becomes irrelevant.

3. Results and discussion

3.1 Explicit MD

To validate the new boundary condition, it is tested in a MD simulation of an Argon gas between a hot and a cold wall. The argon molecules were simulated with a Lennard-Jones

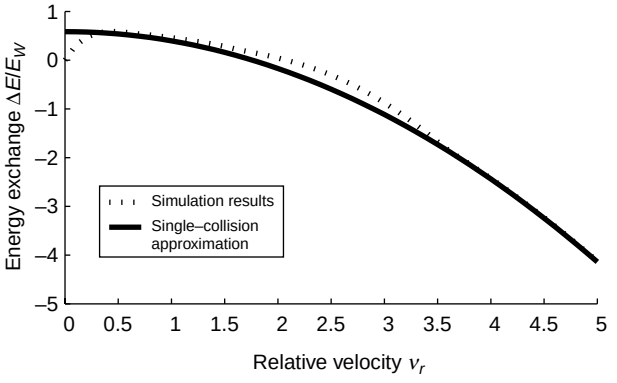

Figure 6. Mean total energy exchange in collisions. The solid line shows the result from (26) in which only single collisions are taken into account, the dashed line shows MD simulation results in which multiple collisions can occur, the mass ratio $\mu = 3.6$.

potential with molecular diameter $\sigma_{\mathrm{Ar}} = 0.340\,\mathrm{nm}$, potential well depth $\varepsilon_{\mathrm{Ar}}/k_{\mathrm{B}} = 121\,\mathrm{K}$ [18] and mass $m_{\mathrm{Ar}} = 6.63 \times 10^{-26}\,\mathrm{kg}$. The calcium wall is approximated as Lennard-Jones substance with molecular diameter $\sigma_{\mathrm{Ca}} = 0.360\,\mathrm{nm}$, mass $m_{\mathrm{Ca}} = 6.65 \times 10^{-26}\,\mathrm{kg}$ and potential well depth $\varepsilon_{\mathrm{Ca}}/k_{\mathrm{B}} = 2497\,\mathrm{K}$ [19]. The interaction between argon and calcium is by a Lennard-Jones potential with $\varepsilon_{\mathrm{Ar-Ca}}/k_{\mathrm{B}} = \varepsilon_{\mathrm{Ar}}/k_{\mathrm{B}} = 121\,\mathrm{K}$. The simulation uses two walls of 18,000 calcium particles each, with 28,154 argon particles placed in two sections between them. Each section has a size of $32 \times 46.9 \times 46.9\ \sigma_{\mathrm{Ar}}^3$, so the volume is $70,387\ \sigma_{\mathrm{Ar}}^3 = 2767\,\mathrm{nm}$. With 14,077 gas particles per section, the gas density is $n = 0.2\,m_{\mathrm{Ar}}/\sigma_{\mathrm{Ar}}^3 = 338\,\mathrm{kg\,m^{-3}}$, and the Knudsen number $Kn = 0.027$, so a continuum approximation should still work well. One calcium wall is initially 'hot', $T_h = 240\,\mathrm{K}$, the other is 'cold', $T_c = 120\,\mathrm{K}$ and the argon has an initial uniform temperature $T_g = 180\,\mathrm{K}$. First, the simulation is allowed to reach an equilibrium with Berendsen thermostats [20] on both walls, so that they maintain their temperature. Then, the thermostats are removed and the temperature developed is calculated. The temperatures of the hot wall and the cold wall converge to 180 K in several 100 ns.

3.2 MD simulation with vibrating potential wall

To test the model with the vibrating walls, simulations of particles interacting with a vibrating potential wall were performed, according to the model from Figure 4(b) and relation (24). The simulation described above was done again, with the same number of argon gas particles, but the walls were replaced by the new model, according to Figure 7.

The total wall energy E_{wall} is related to the wall energy T_w by the assumption that all 18,000 wall particles have a mean energy (kinetic and potential) of $3k_{\mathrm{B}}T$. Similar to the explicit wall, the temperatures of the hot wall and the cold wall converge to 180 K in several 100 ns. The temperature development for the explicit wall simulation and for the implicit wall simulation is compared in Figure 8.

These results were achieved in different simulation times; the explicit wall simulation lasted about 70 h, whereas the simulation with the new boundary condition needed about 10 h on a single processor.

Although the linear relation (24) appears to be a good approximation over a large parameter region, it is not exact, and can differ for certain values of δ and λ, so the model might not work for special situations outside the scope of this research. Furthermore, the derivation of (24) is based on an ideal gas, and the numerical parameter in (23) has been fitted from a model with only one particle and a wall, whereas in real situations the fluid can be far from ideal, and more particles can simultaneously interact with the wall. The good agreement of time scale

Downloaded by [Eindhoven Technical University] at 00:39 07 October 2011

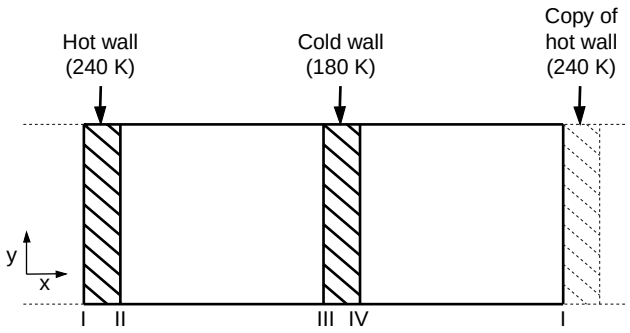

Figure 7. Simulation set-up with new boundary conditions: at (I) and (II) vibrating reflective walls with mass $9000\,m_{\mathrm{Ca}}$ and initial temperature 120 K, at (III) and (IV) vibrating reflective walls with mass $9000\,m_{\mathrm{Ca}}$ and initial temperature 240 K. The temperature of the hot wall is defined as the mean temperature between (I) and (II), and the temperature of the cold wall is defined as the mean temperature between (III) and (IV). Periodic boundary conditions are used in all directions, such that all the walls are infinitely large, and there is a copy of the hot wall on the right of the cold wall.

in Figure 8 suggests that the heat exchange of the more complex explicit wall is still predicted accurately by the model based on the vibrating wall.

3.3 MD simulation with vibrating reflective walls

The reflective wall boundary condition was analysed with a similar set-up as the potential wall, only at lower density. This was done as the reflective wall ignores the potential energy contribution of the interaction between wall and gas, and this contribution is the lowest at low density. In total, 1300 argon gas molecules were used here, this corresponds to a density of $31.2\,\mathrm{kg\,m^{-3}}$, and a Knudsen number of $Kn = 0.37$. Similar to the potential wall analysis, the gas was first allowed to reach equilibrium, and a temperature gradient in the gas developed. After that, the thermostats that kept the walls at their initial temperature were removed, and the temperature developments of the walls were compared.

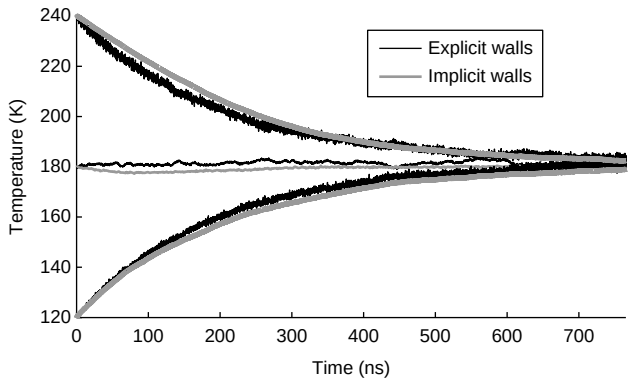

Figure 8. The temperature development of a hot wall (starting at $T = 240\,\mathrm{K}$), a cold wall (starting at $T = 120\,\mathrm{K}$) and the gas (starting at average temperature $T = 180\,\mathrm{K}$) in the complete MD simulation compared with the temperature development of the MD simulation with the new boundary condition. The initial gas density in both simulations is $n = 0.2\,m_{\mathrm{Ar}}/\sigma_{\mathrm{Ar}}^3 = 338\,\mathrm{kg\,m^{-3}}$.

The results for the simulations done with explicit walls and with the newly developed boundary condition are shown in Figure 9(a). The results are similar; the temperature development is the same in the simulation with the vibrating reflective wall boundary conditions as in the simulation with the explicit walls.

To check the sensitivity in the mass ratio μ, the simulation was done again with $\mu = 8$. After 4.3 μs, the temperatures of the cold and hot walls were 150 and 212 K, respectively, compared with 141 and 223 K with mass ratio $\mu = 3.6$. Because a change in mass ratio of more than 100% results in a change in temperature of only around 5–10%, the sensitivity on parameter μ is low.

The situation is also shown for a variation of the diffusive-specular model [21]. Because the standard diffusive-specular model prescribes a constant wall

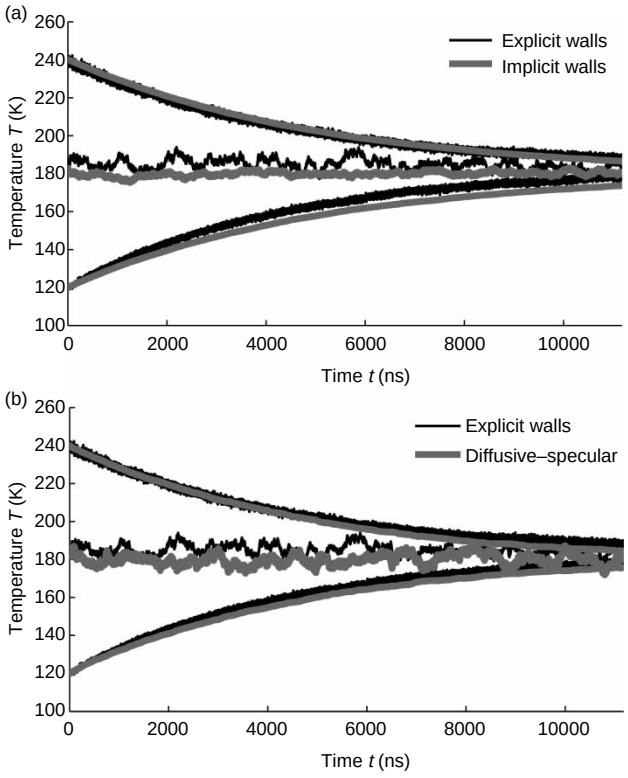

Figure 9. Temperature development of a hot wall (starting at $T = 240\,\mathrm{K}$) and a cold wall (starting at $T = 120\,\mathrm{K}$), both of mass $18,000\,m_{\mathrm{Ca}}$, with a gas with mean temperature $T = 180\,\mathrm{K}$ and 1300 particles with mass m_{Ar} in between. Left panel: explicit walls (solid lines) and vibrating reflective wall boundary conditions (grey line); right panel: explicit walls (solid lines), diffusive-specular boundary conditions with fitted accommodation coefficient $\alpha = 0.05$ (grey line).

Downloaded by [Eindhoven Technical University] at 00:39 07 October 2011

temperature, the model was adapted to a varying wall temperature, by keeping the total energy in the system constant, such that in a collision between a gas particle and the wall, the change in kinetic energy of the particle became equal to the change in thermal energy in the part of the wall that was affected by the collision. By trial and error, the accommodation coefficient was fitted at $\alpha = 0.5$, for which the results are shown in Figure 9(b). The accommodation coefficient is high in comparison with the earlier mentioned value $\alpha = 0.12$ in Ref. [22], probably due to a lower density or varying wall temperature. The accommodation coefficient is not a constant value, but depends on the temperature; so, in a different situation a different accommodation coefficient is needed that might not be a priori known.

The simulation with explicit wall and with a boundary condition at the wall differs in calculation time. Both simulations with vibrating reflective and with diffusive-specular walls were more than 60 times faster than the full MD simulation, in which all computations were performed with the MD-code PumMa.

3.4 Discussion

The computation times for the explicit wall simulation and the simulation with the vibrating wall model are compared in Table 1. In general, the computation time at lower density is smaller because there are less particles. At lower density, the new model decreases the simulation time by a factor of 60, whereas at higher density it is only decreased by a factor of 6; this is because at a lower density, the contribution of the wall to the calculation time is relatively high, so relatively more time can be saved by eliminating the need to calculate their positions.

The heat transfer P_b between the vibrating wall and the fluid according to both (24) and (26) corresponds to the granular media result of $P_b = pVLf(U/V)$ [23], where f is, respectively, given by

$$f\frac{U}{V} = \frac{2\mu^2}{(1+\mu)^2}\sqrt{\frac{3}{2\pi}}\left(\frac{V}{U} - \frac{U}{V}\right),$$
$$f\frac{U}{V} = \frac{2\mu^2}{(1+\mu)^2}\sqrt{\frac{3}{2\pi}}\left(\left(1 - \frac{1}{2\mu}\right)\frac{V}{U} - \frac{U}{2V}\right). \tag{27}$$

Table 1. Computation times of MD simulations of argon at different densities with different walls, simulating 765 ns on 1 CPU.

Average gas density (kg m^{-3})	Explicit walls	Vibrating potential walls	Vibrating reflective walls
338	70 h	10 h	–
31.2	13 h, 3 min	11 min	12 min

This is close to the result for infinitely massive walls ($\mu \to \infty$), for which $f(U/V) = V/U$.

Because in the vibrating wall model only the velocity components of the gas particles normal to the wall are affected, the vibrating wall model presented above cannot be used to model the slip velocity, for this a modification of the theory is needed. Because the particles moving away from the wall exchange some energy with the wall, their energy levels are different from those of the particles going towards the wall; this results in a temperature jump.

4. Conclusions

The heat transfer in MD between solid and fluid was simplified by analysing the solid wall as a vibrating rigid particle with finite mass. On the basis of this model, the energy transfer from the wall to the particle was predicted for a potential wall and a reflective wall. This is used as an implicit boundary condition that replaces the explicit wall. Both results were tested by MD simulations of explicit walls and implicit walls. The implicit wall gives the same results as the explicit wall, in a simulation time that is up to 60 times smaller.

The heat transfer with the vibrating wall model is comparable with that with the explicit wall model, as no parameters had to be fitted for this result, which puts the method above the diffusive-specular model, in which the accommodation coefficient has to be known. The only parameter in the model, the mass ratio μ between a particle and the interacting part of the wall, is known from the literature results, and has only a minor influence on the results.

Acknowledgements

Appreciation is expressed to S.V. Nedea, A.J. Markvoort and P. Spijker for useful suggestions during several discussions. This work was financially supported by MicroNed grant 4-A-6.

References

[1] R. Schmidt and B. Notohardjono, *High-end server low-temperature cooling*, IBM J. Res. Dev. 46 (2002), pp. 739–751.
[2] Semiconductor Industry Association, The International Technology Roadmap for Semiconductors 2010 [online]. Available at http://www.itrs.net/home.html.
[3] F. Incropera and D. DeWitt, *Fundamentals of Heat and Mass Transfer*, Wiley, New York, 2001.
[4] W. Kuan and S. Kandlikar, *Experimental study and model on critical heat flux of refrigerant-123 and water in microchannels*, J. Heat Transfer 130 (2008), p. 034503.
[5] P. Stephan and J. Hammer, *A new model for nucleate boiling heat transfer*, Wärme- und Stoffübertragung 30 (1994), pp. 119–125.
[6] G.A. Bird, *Molecular Gas Dynamics and the Direct Simulation of Gas Flows*, Clarendon Press, Oxford, 1994.
[7] M.P. Allen and D.J. Tildesley, *Computer Simulation of Liquids*, Oxford University Press, Oxford, 1989.
[8] D. Frenkel and B. Smit, *Understanding Molecular Simulations: From Algorithms to Applications*, Academic Press, San Diego, CA, 1996.

[9] C. Cercignani, *Mathematical Methods in Kinetic Theory*, Springer, New York, 1988.
[10] S. Nedea, A. Markvoort, P. Spijker, and A. van Steenhoven, *Heat transfer predictions using accomodation coefficients for a dense gas in a micro/nano-channel*, in *ICNMM2008*, ASME, Darmstadt, Germany, 2008, p. 62179.
[11] A. Markvoort, K. Pieterse, M. Steijaert, P. Spijker, and P. Hilbers, *The bilayer-vesicle transition is entropy driven*, J. Phys. Chem. B 109 (2005), pp. 22649–22654.
[12] A. Leach, *Molecular Modelling – Principles and Applications*, 2nd ed., Prentice Hall, Harlow, 2001.
[13] R.L.C. Vink, G.T. Barkema, W.F. van der Weg, and N. Mousseau, *Fitting the Stillinger–Weber potential to amorphous silicon*, J. Non-Cryst. Sol. 282 (2001), pp. 248–255.
[14] M. van Beek, C. Rindt, J. Wijers, and A. van Steenhoven, *Rebound characteristics for 50-μm particles impacting a powdery deposit*, Powder Technol. 165 (2006), pp. 53–64.
[15] J. Jeans, *The Dynamic Theory of Gases*, Dover Publications, New York, 1954.
[16] P. Atkins and J. de Paula, *Physical Chemistry*, 7th ed., Oxford University Press, Oxford, 2002.
[17] S. Volz and G. Chen, *Molecular dynamics simulation of thermal conductivity of silicon crystals*, Phys. Rev. B 61 (2000), pp. 2651–2656.
[18] S. Maruyama, *Molecular Dynamics Methods in Microscale Heat Transfer*, ch. 2.13.7, Begell House, New York, 2004.
[19] A. Markvoort, P. Hilbers, and S. Nedea, *Molecular dynamics study of the influence of wall-gas interactions on heat flow in nanochannels*, Phys. Rev. E 71 (2005), pp. 066702-1–066702-9.
[20] H.J.C. Berendsen, J.P.M. Postma, W.F. van Gunsteren, A. DiNola, and J.R. Haak, *Molecular dynamics with coupling to an external bath*, J. Chem. Phys. 81 (1984), pp. 3684–3690.
[21] K. Yamamoto, H. Takeuchi, and T. Hyakutake, *Characteristics of reflected gas molecules at a solid surface*, Phys. Fluids 18 (2006), p. 046103.
[22] S. Nedea, A. Markvoort, A. van Steenhoven, and P. Hilbers, *Heat transfer predictions for micro-/nanochannels at the atomistic level using combined molecular dynamics and Monte Carlo techniques*, J. Heat Transfer 131 (2009), p. 033104.
[23] S. McNamara and S. Luding, *Energy flows in vibrated granular media*, Phys. Rev. E 58 (1998), pp. 813–822.

Downloaded by [Eindhoven Technical University] at 00:39 07 October 2011